Mathematical modelling of canonical and non-canonical NF-κB pathways in TNF stimulation

Bing Ji[1], Yao Zhang[2], Changqing Zhen[3], Michael J Fagan[4], Qing Yang[5]

1. School of Control Science and Engineering, Shandong University, Jinan, 250061, P.R. China

2. School of Control Science and Engineering, Shandong University, Jinan, 250061, P.R. China

3. Department of Hematology, Shandong Provincial Hospital Affiliated to Shandong First Medical University, Jinan 250021, P.R. China

4. School of Engineering, University of Hull, Hull, HU6 7RX, UK

5. Department of Breast and Thyroid Surgery, Shandong Provincial Hospital Affiliated to Shandong First Medical University, Jinan, 250021, P.R. China

Running title: Mathematical modelling of NF-κB pathway in TNF stimulation

Corresponding author:

Dr. Qing Yang
Shandong Provincial Hospital Affiliated to Shandong First Medical University
Jinan
250021
P.R. China

Tel: 0086 531 88396813
Fax: 0086 531 88396813
Email: qyangsdu@hotmail.com

ABSTRACT

Background and Objective: NF-κB can be activated by the canonical and non-canonical pathways. These two pathways interplay via the TRAF1|NIK complex after stimulation by TNF. However existing mathematical models of two pathways are inadequate. In this context, an improved mathematical model is constructed to simulate these two pathways and their coupling stimulated by TNF.

Methods: A schematic description of two NF-κB pathways and their relation after TNF stimulation is constructed at first. Then twenty-eight ordinary differential equations are utilized to build the mathematical model. Model equations are solved via the ordinary differential equation solver (ode23).

Results: The proposed model firstly reconstructs the changes in concentrations of NF-κB pathway related biochemical factors with time, and further investigates the underlying mechanism of interaction between two pathways through the TRAF1|NIK complex after stimulation.

Conclusions: The model is validated through good agreement between simulation results and published experimental observations. This study helps to well understand the canonical and non-canonical pathways and their interaction. It also provides a potential tool to investigate how the dysregulated pathways act in pathological conditions.

KEY WORDS: NF-κB; Canonical pathway; Non-canonical pathway; Coupling; Mathematical modelling

1. INTRODUCTION

The mammalian nuclear factor-kappa B (NF-κB) includes five transcription factors: NF-κB1(p50/p105), NF-κB2(p52/p100), RelA(p65), RelB and cRel [1-3]. These five factors are able to form homo-or heterodimers with each other [4]. Specially, p50 and p65 form p50|p65 heterodimers acting in the canonical pathway, while p52|RelB heterodimers formed by p52 and RelB, take part in the non-canonical pathway [5, 6].

NF-κB always stays in un-stimulated state in the cytoplasm by inhibitors, such as IκBα in resting cells [7]. NF-κB can be activated via the canonical and non-canonical signalling pathways [8-10]. The canonical pathway mainly involves IκBα being targeted for degradation by the cytoplasmic IκBα kinase (IKK). IKK can phosphorylate, ubiquitinate and thereby target IκBα for degradation, consequently decomposing the complex of IκBα|NF-κB and further releasing NF-κB (p50|p65) [11,12]. The key point in the non-canonical pathway is p100 transformed into p52 under mediation of NF-κB-inducing kinase (NIK), which then forms p52|RelB heterodimers with RelB [13, 14]. As an essential part of the NF-κB pathway, the non-canonical pathway acts important functions in many biological processes and its abnormalities is reported to linked to several malignancies [5].

Despite NF-κB pathway being such an important biological process, it has not been completely elucidated. Hence mathematical models, proven to be an auxiliary method for studying complicated biological processes [15-18], have been proposed to mimic NF-κB signalling pathways [1, 6, 16, 19-22]. However, as far as we know, these previous models mainly focused on the canonical pathway, but did not consider the non-canonical pathway, with the exception of the work of Choudhary et al. [23]. Although the study of [23] simulated both NF-κB pathways, we noted several significant inconsistencies exists. The details are included in Appendix A. In this

context, an extended mathematical model is constructed in this paper to mimic the canonical as well as non-canonical pathway, further investigate the underlying coupling mechanism of two pathways.

2. METHODS

Figure 1 shows a schematic description of two NF-κB pathways and the relation between them after TNF stimulation. As demonstrated in Figure 1, the left part of Figure 1 presents functions of the canonical pathway. p50|p65 always stays in un-stimulated state in the cytoplasm by several inhibitors in resting cells [1, 4, 24]. These NF-κB inhibitors named IκBs, include IκBα, IκBβ, IκBγ and IκBε, are able to bind to p50|p65, and then suppress its activities [24]. Considering p50|p65 is primarily suppressed by IκBα, this model only considers IκBα for simplicity. IKK serves as an activator for the canonical pathway and usually stays in neutral state (denoted by IKKn) in resting cells [25]. TNF can trigger the transformation of IKKn into its active state (denoted by IKKa). IKKa is able to phosphorylate and ubiquitinate IκBα, targeting it for destruction, consequently releasing free p50|p65 heterodimers. The released p50|p65 can quickly move into the nucleus from the cytoplasm and bind to gene promoters on DNA to express genes such as IκBα, A20, TRAF1, TRAF2, TRAF3 and p100 [26]. Among these newly produced proteins, IκBα and A20 serve as two inhibitors of the canonical pathway [1, 4]. They can limit the canonical pathway in different ways and thus trigger a negative feedback loop. Thus, IκBα moves into the nucleus from the cytoplasm to inactivate p50|p65 heterodimers and initiate their translocation back to the cytoplasm. In addition, A20 can promote the transformation of IKKa into its un-activated state (denoted as IKKi in our model). IKKi cannot phosphorylate IκBα [1, 27]. It should be noted that although IKK are transformed among three states (IKKn, IKKa and IKKi), the total amount of IKK keeps nearly constant.

The right part of Figure 1 demonstrates underlying mechanisms of the activation of the non-canonical pathway as well as coupling between two pathways [23]. NIK acts as an important biochemical factor in activating the non-canonical signalling, Its concentration is always limited at a rather low level by the TNF receptor-associated factor3 (TRAF3) in the TRAF2|cIAP1/2 complex in resting cells [4]. Newly synthesized TRAF1 in the canonical pathway can disturb the ubiquitination of NIK by TRAF3 through forming the TRAF1|NIK complex. The TRAF1|NIK complex can then promote p100 transformation into p52, which is necessary for the non-canonical pathway. p52 forms p52|RelB heterodimers with RelB and moves into the nucleus from the cytoplasm to regulate gene expression.

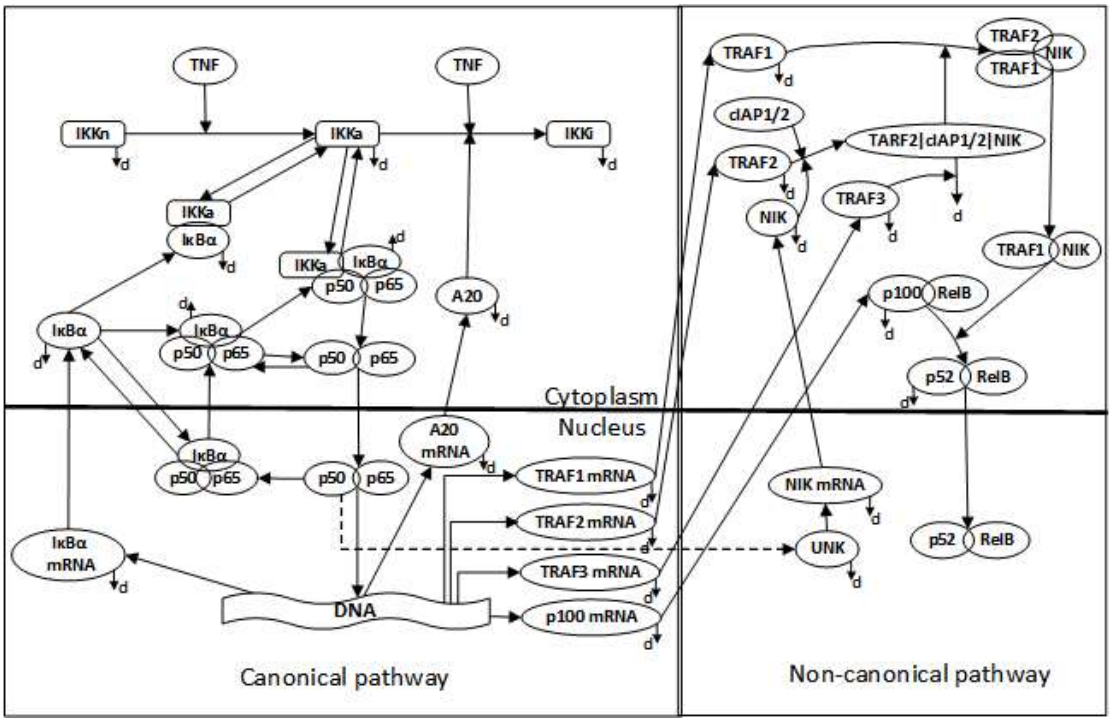

Figure 1: The schematic description of two NF-κB pathways for TNF stimulation. (Note that "d" represents the degradation of biochemical factors).

According to biological fundamentals of two pathways as demonstrated in Figure 1, an extended mathematical models is built to simulate two pathways as well as their interaction. The model totally consists of twenty-eight ordinary differential equations

(ODEs). Following the earlier work of Lipniacki et al. [1], which concentrates on modelling of the canonical pathway, our model utilizes a similar set of fourteen ODEs to mimic the canonical pathway. The details of these ODEs are not repeated here, but included as equations (B.1) - (B.14) in Appendix B for convenience. In this context, this work mainly focuses on building another fourteen ODEs to simulate the non-canonical pathway and the interaction between two pathways. The details of these newly proposed ODEs are presented as follows:

$$\frac{d}{dt}TRAF1_t(t) = n_{1e} + n_{1a}p50_n(t) - n_{1c}TRAF1_t(t) \quad (1)$$

$$\frac{d}{dt}TRAF1(t) = n_{1b}TRAF1_t(t) - b_3TRAF1(t)(TRAF2|NIK)(t) - n_{1d}TRAF1(t) \quad (2)$$

$$\frac{d}{dt}TRAF2_t(t) = n_{2e} + n_{2a}p50_n(t) - n_{2c}TRAF2_t(t) \quad (3)$$

$$\frac{d}{dt}TRAF2(t) = n_{2b}TRAF2_t(t) - b_1TRAF2(t)NIK(t) - n_{2d}TRAF2(t) \quad (4)$$

$$\frac{d}{dt}NIK_t(t) = n_{3d} + n_{3a}UNK(t) - n_{3c}NIK_t(t) \quad (5)$$

$$\frac{d}{dt}NIK(t) = n_{3b}NIK_t(t) - b_1TRAF2(t)\mathrm{NIK(t)} - n_{4d}NIK(t) \quad (6)$$

$$\frac{d}{dt}(TRAF2|NIK)(t) = b_1TRAF2(t)NIK(t) - b_2(TRAF2|NIK)(t) - b_3TRAF1(t)(TRAF2|NIK)(t) \quad (7)$$

$$\frac{d}{dt}(TRAF1|TRAF2|NIK)(t) = b_3TRAF1(t)(TRAF2|NIK)(t) - b_4(TRAF1|TRAF2|NIK)(t) \quad (8)$$

$$\frac{d}{dt}(TRAF1|NIK)(t) = b_4(TRAF1|TRAF2|NIK)\mathrm{(t)} - nc_5p100(t)(TRAF1|NIK)(t) \quad (9)$$

$$\frac{d}{dt}p100_t(t) = nc_6 + nc_1p50_n\mathrm{(t)} - nc_3p100_t(t) \quad (10)$$

$$\frac{d}{dt}p100(t) = nc_2p100_t(t) - nc_4p100(t) - nc_5p100(t)(TRAF1|NIK)\mathrm{(t)} \quad (11)$$

$$\frac{d}{dt}p52(t) = nc_5p100(t)(TRAF1|NIK)(t) - nc_7p52(t) + nc_8p52_n(t) - nc_9p52(t) \quad (12)$$

$$\frac{d}{dt}p52_n(t) = nc_7p52(t) - nc_8p52_n(t) \quad (13)$$

$$\frac{d}{dt}UNK(t) = n_{4e} + n_{4a}p50_n(t) - n_{4c}UNK(t) \quad (14)$$

Equations (1) - (14) describe the variation in amounts of mRNAs, proteins and complexes involved in the non-canonical pathway with time, respectively. As an

example, $\frac{\mathrm{d}}{\mathrm{dt}}\mathrm{TRAF1_t(t)}$ is the variation of $\mathrm{TRAF1_t}$ with time as demonstrated in equation (1). n_{1e} represents the synthesis of constitutive TRAF1 mRNA. n_{1a} represents the synthesis of TRAF1 mRNA induced by $\mathrm{p50_n}$. n_{1c} represents the degradation rate of TRAF1 mRNA. Equations (1), (3), and (10) all involve p50n. Since p50n is produced in the canonical pathway, the definition of the variation in p50n concentration is included in equation (B.7) in Appendix B. Considering that factors which induce the synthesis of NIK mRNA are currently not completely understood, for simplicity, it is assumed here that NIK gene transcription is regulated by an unknown promoter denoted by UNK in equation (5) as also suggested by Choudhary et al. [23]. As shown in equation (14), the amount of UNK is assumed to be regulated by p50n. The definitions of variables used in the model are listed in Table 1. The details of model parameters are listed in Table 2. In these tables, experimental data of n_{1a} and n_{1c} are not available, and thus their values are fitted via a Genetic Algorithm. n_{1a} and n_{1c} are set as inputs of GA, while the increasing fold changes in TRAF1 mRNA and TRAF2 mRNA after TNF stimulation are set as outputs. However, more biological research is require to identify the exact levels of the fold change. Here, the fold change is set as 36. More detailed information of GA is included in Appendix C.

Variable	**Description**
$TRAF1_t$	The amount of TRAF1 mRNA
$TRAF1$	The amount of TRAF1 protein
$TRAF2_t$	The amount of TRAF 2 mRNA
$TRAF2$	The amount of TRAF2 protein

Table 1: Definitions of variables used in the model.

Variable	Description
NIK_t	The amount of NIK mRNA
NIK	The amount of NIK protein
TRAF2 | NIK	The amount of complexes of TRAF2 and NIK
TRAF1 | TRAF2 | NIK	The amount of complexes of TRAF1, TRAF2 and NIK
TRAF1 | NIK	The amount of complexes of TRAF1 and NIK
$p100_t$	The amount of p100 mRNA
$p100$	The amount of cytoplasmic $\mathrm{p100}$ protein
$p52$	The amount of p52 in the cytoplasm
$p52_n$	The amount of p52 in the nucleus
$p50_n$	the nuclear concentration of $\mathrm{p50}$ protein produced in the canonical NF-κB pathway
UNK	the amount of UNK in the nucleus

Table 1 (cont): Definitions of variables used in the model.

Symbol	Values	Units	Description	Comments
n_{1a}	7×10^{-8}	s^{-1}	TRAF1-inducible mRNA synthesis	Fitted
n_{1b}	0.5	s^{-1}	TRAF1 translation rate	[23]
n_{1c}	4.62×10^{-5}	s^{-1}	TRAF1 mRNA degradation	Fitted
n_{1d}	0.0003	s^{-1}	TRAF1 degradation rate	[23]

Table 2: Definitions and values of model parameters.

Symbol	Values	Units	Description	Comments
n_{1e}	0.0	μMs^{-1}	TRAF1-constitutive mRNA synthesis	[23]
n_{2a}	5×10^{-7}	s^{-1}	TRAF2-inducible mRNA synthesis	[23]
n_{2b}	0.5	s^{-1}	TRAF2 translation rate	[23]
n_{2c}	0.0004	s^{-1}	TRAF2 mRNA degradation	[23]
n_{2d}	0.0003	s^{-1}	TRAF2 degradation rate	[23]
n_{2e}	0.0	μMs^{-1}	TRAF2-constitutive mRNA synthesis	[23]
n_{3a}	3.75×10^{-8}	s^{-1}	NIK-inducible mRNA synthesis	Assumption
n_{3b}	0.5	s^{-1}	NIK translation rate	[23]
n_{3c}	0.0004	s^{-1}	NIK mRNA degradation	[23]
n_{3d}	0.0	μMs^{-1}	NIK-constitutive mRNA synthesis	[23]
n_{4a}	1.2	s^{-1}	UNK-inducible synthesis	Assumption
n_{4d}	0.0003	s^{-1}	NIK degradation rate	Assumption
n_{4c}	1.0	s^{-1}	UNK degradation	Assumption
n_{4e}	0.0	μMs^{-1}	UNK-constitutive synthesis	Assumption
b_1	1.0	s^{-1}	TRAF2-NIK association	[23]
b_2	6.42×10^{-5}	s^{-1}	NIK and TRAF1 degradation from TRAF2-NIK complex	[23]

1 Table 2 (cont): Definitions and values of model parameters.

2

Symbol	Values	Units	Description	Comments
b_3	0.5	s^{-1}	TRAF1 association with TRAF2-NIK complex	[23]
b_4	0.25	s^{-1}	formation of TRAF1-NIK complex by displacing TRAF2 from TRAF2-NIK complex	[23]
nc_1	2.5×10^{-8}	s^{-1}	p100-inducible mRNA synthesis	[33]
nc_2	0.5	s^{-1}	p100 translation rate	[23]
nc_3	3.2×10^{-5}	s^{-1}	p100 mRNA degradation	[33]
nc_4	0.0004	s^{-1}	p100 degradation rate	[23]
nc_5	0.002	s^{-1}	TRAF1-NIK and p100 association	[23]
nc_6	0.0	μMs^{-1}	p100-constitutive mRNA synthesis	[23]
nc_7	7.5×10^{-4}	s^{-1}	p52 nuclear import	[33]
nc_8	0.0002	s^{-1}	p52 nuclear export	[33]
nc_9	3.2×10^{-5}	s^{-1}	p52 degradation rate	Assumption

Table 2 (cont): Definitions and values of model parameters.

3. RESULTS

The proposed model equations above are solved by the ordinary differential equation solver (ode23) with the initial values of model variables as shown in Table 3. The initial values in Table 3 refer to steady values of the biochemical factors with regard to the NF-κB pathway without TNF stimulation. These values are derived following such way:

given a group of randomly chosen values of state variations (representing concentrations of the biochemical factors), the concentrations of related biochemical factors will vary and finally achieve a steady state without TNF stimulation. The code implementation was performed via the Matlab language (R2018b, The MathWorks, Inc, Natick, USA). The corresponding MATLAB codes are included in supplementary data. Considering that model simulation of the canonical NF-κB pathway has been performed as discussed in section 2 [1], thereby the corresponding simulation results are not presented in this section, but demonstrated in Appendix B. This section mainly demonstrates simulation results of the non-canonical pathway and the interaction between two pathways.

Variable	**Initial value**	**Units**
TRAF1 mRNA	3.48×10^{-6}	μM
TRAF2 mRNA	2.87×10^{-6}	μM
TRAF1	0.0054	μM
TRAF2	0.0044	μM
NIK mRNA	2.58×10^{-7}	μM
NIK	2.76×10^{-5}	μM
TRAF2 | NIK	4.37×10^{-5}	μM
TRAF1 | TRAF2 | NIK	4.72×10^{-7}	μM
TRAF1 | NIK	1.15×10^{-6}	μM
p100 mRNA	1.79×10^{-6}	μM
p100	0.0022	μM

Table 3: Initial values for the model variables.

Variable	Initial value	Units
p52	$1.61x\ 10^{-7}$	μM
p52n	$6.04x\ 10^{-7}$	μM
p50n	0.0023	μM
UNK	0.0028	μM

Table 3 (cont): Initial values for the model variables.

Figure 2 describe the variations of biochemical factors involved the non-canonical pathway with time and their concentrations are normalized by their initial values (as demonstrated in Table 3 and TNF concentration was set as 1 μM following the work of Lipniacki et al. [1]). Specially, Figure 2A and Figure 2B illustrate the variations in the concentrations of TRAF1 mRNA, TRAF2 mRNA and their proteins with time, respectively. Figure 2C and Figure 2D describes the variations in the concentrations of NIK, TRAF1|NIK complex, TRAF2|NIK complex and TRAF1|TRAF2|NIK complex with time. Figure 2E demonstrates the variations in concentrations of cytoplasmic p100, p52 and the nuclear p52 (p52n) with time. Figure 2F presents the temporal changes in the concentrations of p50n and p52n. Figure 3 to Figure 5 demonstrate influences of TNF variations on the biochemical factors related to the NF-κB pathway.

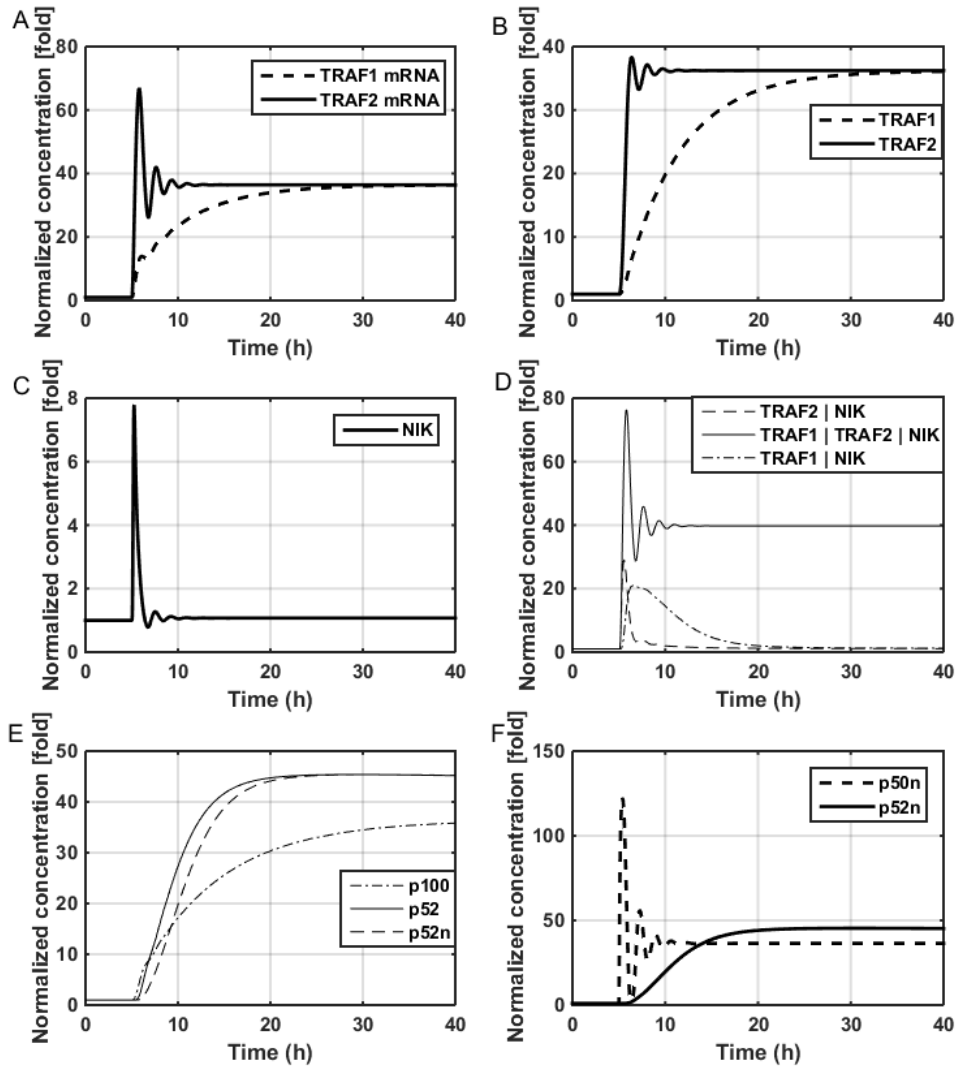

Figure 2: (A) Mimicked changes in the concentrations of TRAF1 mRNA and TRAF2 mRNA with time. (B) Mimicked changes of the variation in the concentrations of TRAF1 and TRAF2 proteins with time. (C) Mimicked changes of variation in the concentration of NIK with time. (D) Mimicked changes of variation in the concentrations of TARF2|NIK, TARF1|NIK and TARF1|TARF2|NIK with time. (E) Mimicked changes of the variation in the concentrations of p100, p52 and p52n with respect to their initial values with time. (TNF stimulation starts at 5th hour). (F) Mimicked changes of the variation in the concentrations of p50n and p52n with time. (TNF stimulation starts at 5th hour).

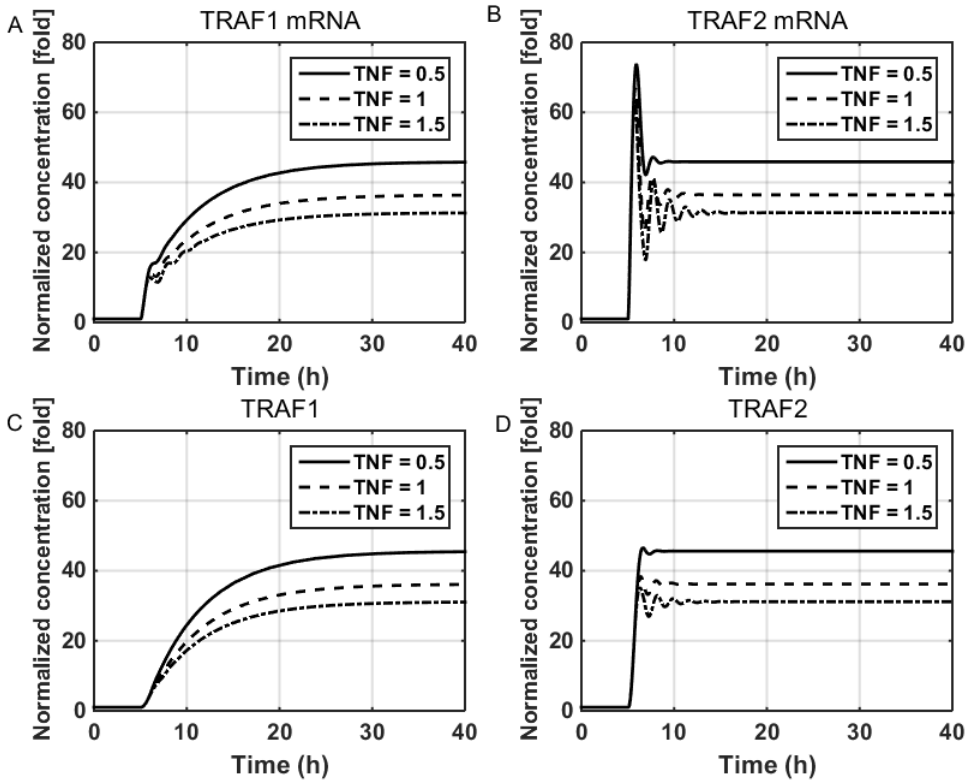

Figure 3: (A) Mimicked changes in the concentration of TRAF1 mRNA with time when TNF are set as 0.5, 1 and 1.5 μM respectively. (B) Mimicked changes in the concentration of TRAF2 mRNA when TNF are set as 0.5, 1 and 1.5 μM respectively. (C) Mimicked changes in the concentration of TRAF1 protein with time when TNF are set as 0.5, 1 and 1.5 μM respectively. (D) Mimicked changes in the concentration of TRAF2 protein with time when TNF are set as 0.5, 1 and 1.5 μM respectively. (TNF stimulation starts at 5th hour).

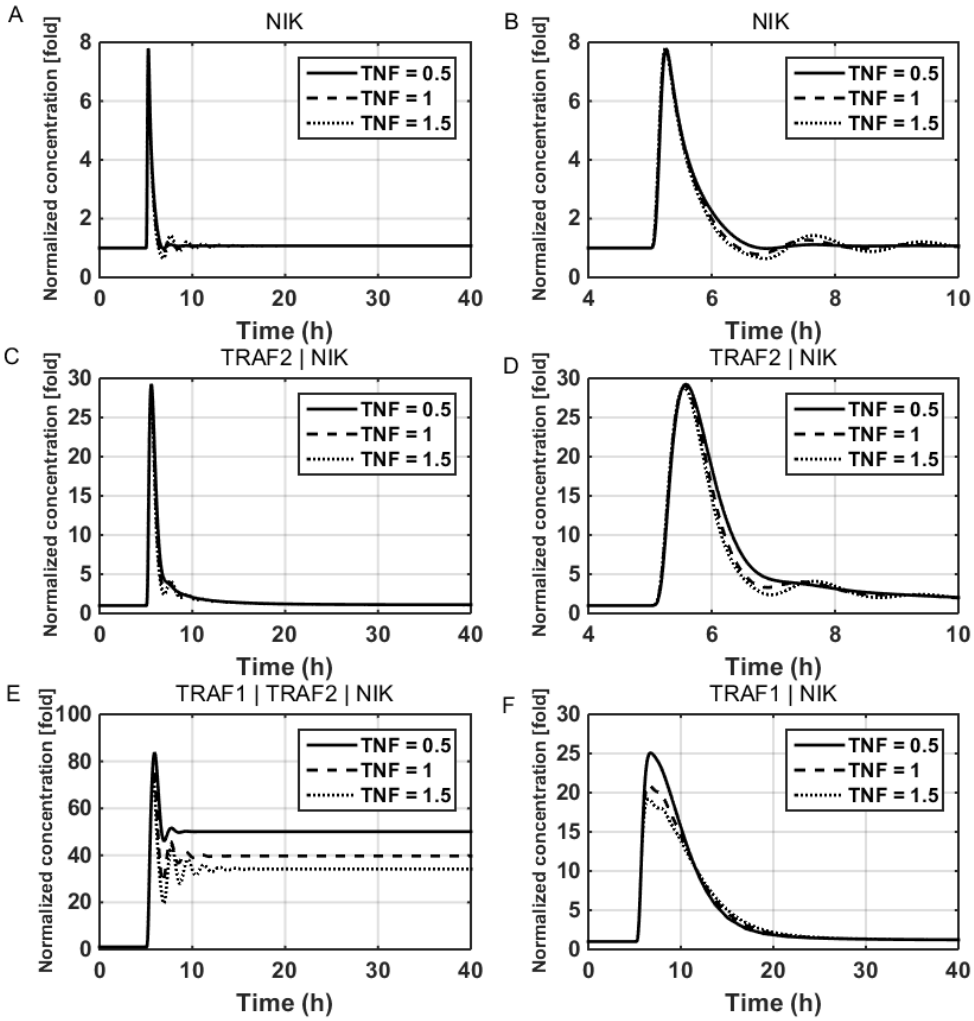

Figure 4: (A) Mimicked changes in the concentration of NIK with time when TNF are set as 0.5, 1 and 1.5 μM respectively. (B) Simulation results demonstrated in (A), but with the short range of the abscissa. (C) Mimicked changes in the concentration of TARF2|NIK with time when TNF are set as 0.5, 1 and 1.5 μM respectively. (D) Simulation results demonstrated in (C), but with the short range of the abscissa. (E) Mimicked changes in the concentration of TRAF1|TARF2|NIK with time when TNF are set as 0.5, 1 and 1.5 μM respectively. (F) Mimicked changes in the concentration of TARF1|NIK with time when TNF are set as 0.5, 1 and 1.5 μM respectively. (TNF stimulation starts at 5th hour).

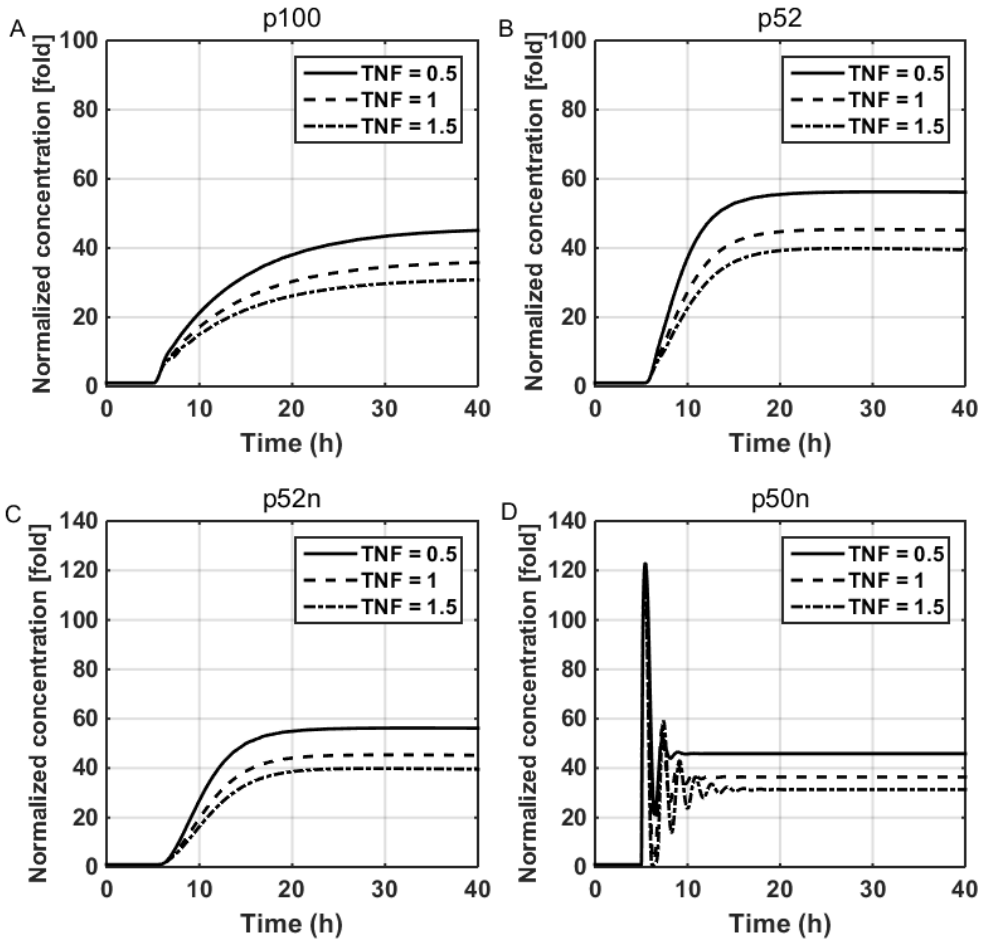

Figure 5: (A) Mimicked changes in the concentration of p100 with respect to its initial value with time when TNF are set as 0.5, 1 and 1.5 μM respectively. (B) Mimicked changes in the concentration of p52 with respect to its initial value with time when TNF are set as 0.5, 1 and 1.5 μM respectively. (C) Mimicked changes in the concentration of p52n with respect to its initial value with time when TNF are set as 0.5, 1 and 1.5 μM respectively. (D) Mimicked changes in the concentration of p50n with time when TNF are set as 0.5, 1 and 1.5 μM respectively. (TNF stimulation starts at 5th hour).

4. DISCUSSION

The simulation results in Figure 2A show that the concentrations of TRAF1 mRNA and TRAF2 mRNA are stable, and stayed at a low level without TNF stimulation during the first four hours. The amounts of TRAF1 mRNA and TRAF2 mRNA begin to increase, and finally reach a new stable state after TNF stimulation starting from 5th hour. These simulation results not only agree with the fact that free p50 released in the canonical

pathway enters the nucleus and then promotes the production of TRAF1 mRNA and TRAF2 mRNA, but are also partially validated by experimental findings of Wang et al. [28], where the experimental observations indicate that TRAF1 mRNA and TRAF2 mRNA both increase during 4 hours after TNF stimulation (the experiment only provided 4 hours' data). As demonstrated in Figure 2B, the stable states of TRAF1 and TRAF2 are disturbed after TNF stimulation (from 5th hour) with a sharp rise in TRAF2 and a gradual rise in TRAF1, which is partially validated by the observations in work of [29] that TRAF1 is upregulated upon TNF stimulation.

As shown in Figure 2C and Figure 2D, the stimulation of TNF disturbs the stable state and triggers a rapid growth of concentrations of NIK, TRAF1|NIK complex, TRAF2|NIK complex and TRAF1|TRAF2|NIK complex. These simulations match the corresponding experimental observations. To be specific, experimental findings indicate that the steady level of NIK protein in resting cells is very low [5]. TNF stimulation promotes the synthesis of NIK by 4 fold initially followed a decrease at 2 hours [30], broadly confirming a 7.5 fold increase and then a decrease in simulation results. Figure 2D shows that TRAF2|NIK undergoes an initial increase and then begins to decrease, while TRAF1|NIK keeps increasing before 6.45 hours. This agrees with the biological fact that NIK is usually held by TRAF2 in the complex, and the increase of NIK can lead to increase in the amount of TRAF2|NIK complex [4]. TRAF1 competes for NIK binding with TRAF2, and consequently TRAF1 produced in the canonical NF-κB pathway leads to a decrease in TRAF2|NIK followed by TRAF1|NIK as shown by the experimental data [23].

The simulation results in Figure 2E demonstrate that p100, p52 and p52n successively increase after TNF stimulation, which agrees with the biological fact that p100 up-regulated by the canonical pathway, is transformed into p52 induced by

TRAF1|NIK complexes and then transported into the nucleus [23]. These simulation results are further confirmed by experimental observations that TNF stimulation can lead to the increase of p100, p52 and p52n [23, 31]. It is should be noted that the higher level of p100 than p52 cannot be observed directly in Figure 2E, due to concentrations of p100 and p52 normalized by their initial values respectively.

As shown in Figure 2F, concentrations of p50n and p52n both initially maintain a stable state, and then undergo an increase due to TNF stimulation. But p50n undergoes an obvious oscillation before achieving a steady state. These model simulations are broadly validated by the experimental observations [6, 23]. In particular, the work of [6] and [23] indicates that p50n increases and achieves a peak value after TNF stimulation at first. Afterwards p50n decreases to a lower value and then switches to increase again. On the other hand, p52n rises and then reaches a steady state, and no obvious oscillations occur. In addition, the model simulations show that p50n increases and reaches a stable state earlier than that of p52n, which agrees with the biological observation that the non-canonical pathway is activated after the canonical NF-κB pathway [23].

Figure 3 to Figure 5 demonstrate influences of TNF variations on the biochemical factors related to the NF-κB pathway. The increase or decrease in TNF leads to the decrease or increase in concentrations of these biochemical factors. However, effects of TNF changes on NIK, TRAF2|NIK and TRAF1|NIK are relatively smaller than the other factors. The sensitivity study of eight of the key model parameters (including c_{6a}, a_1, t_2, i_1, nc_5, nc_7, nc_8 and nc_9) is performed, aiming to investigate the further information of the NF-κB pathway. When the values of parameters are changed between 0.5 and 1.5 with regard to their base values as defined in Table 2, the influences on steady values (normalized to their corresponding values under the condition that TNF is set as 1 μM)

of p50 and p52 are observed. Figure 6 shows how the variations in eight parameters affect p50 concentration. As shown in Figure 6, growths of c_{6a} and t_2 both trigger the increase of p50, whereas the opposite influence is observed with parameters (a_1 and i_1). In addition, the changes of nc_5, nc_7, nc_8 and nc_9 have no effect on p50. Figure 7 indicates the effect of variations in eight parameters on p52 concentration. It can be seen that the increases in c_{6a}, a_1, t_2 and i_1 lead to the increase in p52, while the growth in nc_9 causes the drop of p52. However the changes of nc_5, nc_7 and nc_8 have a negligible effect on p52.

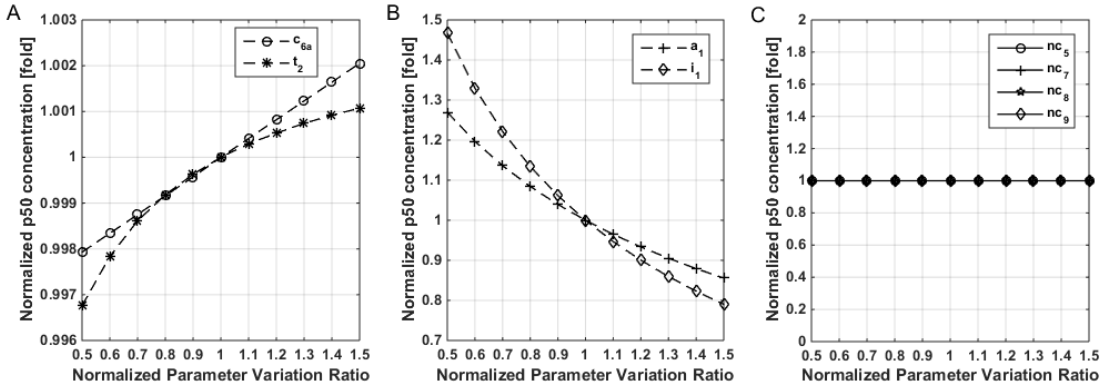

Figure 6: (A) The effect of independently varying each model parameter (c_{6a} and t_2) on the steady concentration of p50. (B) The effect of independently varying each model parameter (a_1 and i_1) on the steady concentration of p50. (C) The effect of independently varying each model parameter (nc_5, nc_7, nc_8 and nc_9) on the steady concentration of p50. p50 concentration is normalized to the value of the base case.

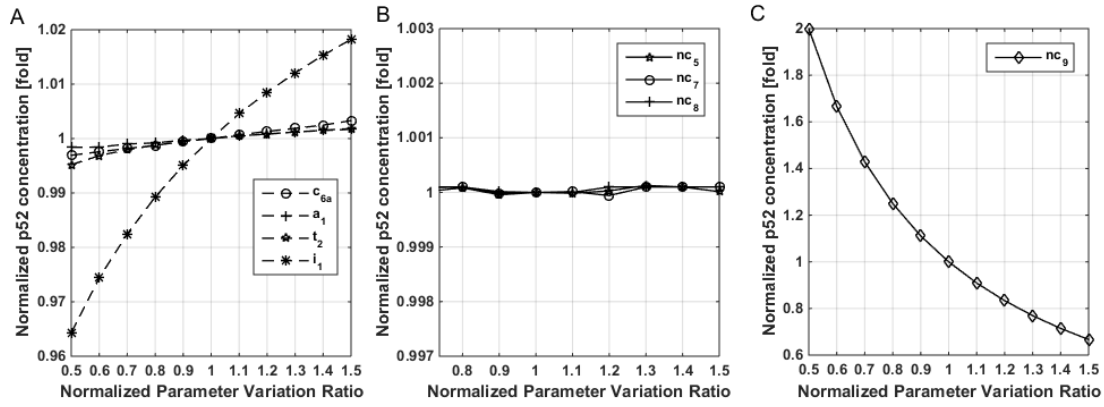

Figure 7: (A) The effect of independently varying each model parameter (c_{6a}, a_1, t_2 and i_1) on the steady concentration of p52. (B) The effect of independently varying each model parameter (nc_5, nc_7 and nc_8) on the steady concentration of p52. (C) The effect of

independently varying each model parameter (nc_9) on the steady concentration of p52. p52 concentration is normalized to the value of the base case.

NF-κB can be activated through the canonical and non-canonical pathways. The non-canonical pathway serves as an essential role in many biological processes, and its dysregulation is related to several malignancies. But the non-canonical pathway was usually ignored in the previous models. As discussed above, the model proposed in this paper mimicked the underlying mechanism of the canonical and the non-canonical pathways, as well as the interaction between them. Then such model was utilized to analyze the experimental observations regarding the canonical and non-canonical pathways.

5. CONCLUSIONS

The non-canonical pathway serving as an important component of the NF-κB pathway, is usually ignored in previously developed mathematical models. Hence the proposed model in this paper extends the work of Lipniacki et al. [1], which only considered the canonical pathway, by adding another fourteen ODEs to include the non-canonical pathway. It should be noted that the specific factors regulating the synthesis of NIK mRNA are not included in the current model as they are still not completely understood. As knowledge of the NF-κB pathway grows, the model can be further refined and optimized to include new observations to produce a more complete simulation and more accurate results.

The NF-κB pathway is un-activated and its associated factors remain in a stable state in resting cells. TNF stimulation can activate the NF-κB pathway and disturb such a stable state with TRAF1 clearly playing a central role in the relation between two pathways. The proposed model not only demonstrates how TNF stimulation triggers the NF-κB pathway and the resultant variation in its associated biochemical factors, but

also investigates the coupling mechanism of two pathways. We believe that this model provides a useful tool to improve our knowledge of the NF-κB pathway and, in particular, how its different components can be deferentially deployed in differing biological contexts. For example, the non-canonical NF-κB pathway is reported to be involved in enhanced osteoclastogenesis occurred in inflammatory arthritis and metastatic bone cancer [4, 32]. This proposed model can be potentially utilized to investigate the role of the non-canonical pathway in the pathogenesis of such diseases.

ACKNOWLEDGEMENT

This work was supported by National Key R&D Program of China [grant 2018YFB1305400]; the National Natural Science Foundation of China [grant number 61673246 and 81301294]; and the Research and Development Program of Jinan [grant number 201907064]. We declare that we have no competing interests. The MATLAB codes for the mathematical model is included in attachment.

APPENDIX A

A1 Apparent inconsistencies in the model developed by Choudhary et al. (2013)

A1.1 Model equations do not agree with the schematic description of the model

Figure 4A in Choudhary et al. (2013) describe the mechanism of both the canonical pathway and non-canonical pathway coupled by TRAF1 dynamics. However, the model built by Choudhary et al. (2013) does not agree with figure 4A. The details are listed as follows:

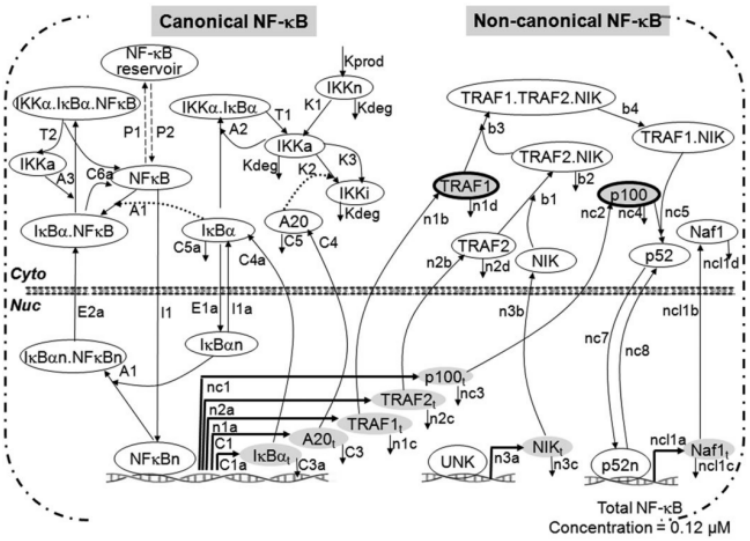

Figure 4A. Schematic description of canonical and non-canonical pathways coupled by TRAF1 [23].

$$\frac{d}{dt}TRAF1(t) = n_{1b}TRAF1_t(t) - n_{1d}TRAF1(t) \quad (2)$$

Figure 4A shows that TRAF1 binding to TRAF2|NIK is involved in the variation of TRAF1, however it is not considered in Equation (2).

$$\frac{d}{dt}TRAF2(t) = n_{2b}TRAF2_t(t) - n_{2d}TRAF2(t) \quad (4)$$

Figure 4A shows that TRAF2 binding to NIK involves in the variation of TRAF2, however again it is not considered in Equation (4).

$$\frac{d}{dt}NIK(t) = n_{3b}NIK_t(t) - b_2(TRAF2|\mathrm{NIK})(t) + b_4(TRAF1|NIK)(t) \quad (6)$$

Figure 4A shows that the degradation of TRAF2|NIK and the formation of TRAF1|NIK are not involved in the variation of NIK directly. However, it is included in Equation (6). On the other hand, the association of NIK and TRAF2 is related to NIK, but is not considered in Equation (6).

$$\frac{d}{dt}(TRAF2|NIK)(t) = b_1TRAF2(t)NIK(t) - b_2(TRAF2|NIK)(t) \quad (7)$$

Figure 4A shows that TRAF2 | NIK binding to TRAF1 is involved in the variation of TRAF2 | NIK, however it is not considered in Equation (7).

$$\frac{d}{dt}(TRAF1|TRAF2|NIK)(t) = b_3 TRAF1(t)(TRAF2|NIK)(t) - b_4(TRAF1|NIK)(t) \quad (8)$$

According to figure 4A, TRAF1|NIK in Equation (8) should be replaced by TRAF1 | TRAF2 |NIK.

$$\frac{d}{dt}p100(t) = nc_2 p100_t(t) - nc_4 p100(t) \quad (10)$$

Figure 4A shows that p100 can transformed into p52 under the regulation of TRAF1 | NIK, but it is not considered in Equation (10).

$$\frac{d}{dt}p52(t) = nc_5 p100(t)(TRAF1|NIK)(t) \quad (11)$$

Figure 4A demonstrates that p52 concentration is influenced by transportation of p52 into and out of the cytoplasm, which is not considered in Equation (11).

In addition, TRAF1 | NIK is involved in Equations (6) and (11). However Choudhary, Kalita et al. (2013) does not define its temporal variation in their model.

A1.2 Model simulation results are inconsistent with model equations

Figure 4B of Choudhary et al. (2013) describes the temporal variation of TRAF1 and TRAF2 after TNF stimulation. However, the simulation results in their figure 4B cannot be produced based on the proposed model of Choudhary et al. (2013). To be specific, as we can see in figure 4B, TRAF1 concentration keeps around zero in the first two hours and then undergoes a rapid decline around the 6th hour. These simulation results do not agree with the model equations.

APPENDIX B

B1 ODEs simulating the canonical NF-κB pathway from Lipniacki et al. (2004)

$$\frac{d}{dt}IKKn(t) = \ _{prod} - \ _{deg}IKKn(t) - T_R \ _1 IKKn(t) \quad (B.1)$$

$$\frac{d}{dt}IKK \ (t) = T_R \ _1 IKKn(t) - \ _3 IKK \ (t) - T_R \ _2 IKK \ (t) \cdot A20(t) - \ _{deg}IKK \ (t)$$

$$- \ _2 IKK \ (t) \cdot I \quad (t) + t_1(IKK \ |I \quad)(t)$$

$$- \ {}_3IKK\ (t) \cdot (I \quad |NF \quad)(t)$$

$$+t_2(IKK\ |I \quad |NF \quad)(t) \tag{B.2}$$

$$\frac{d}{dt} IKK\ (t) = \ {}_3IKK\ (t) + T_R \ {}_2IKK\ (t) \cdot A20(t) - \ {}_{deg}IKK\ (t) \tag{B.3}$$

$$\frac{d}{dt}(IKK\ |I \quad)(t) = \ {}_2IKK\ (t) \cdot I \quad (t) - t_1(IKK\ |I \quad)(t) \tag{B.4}$$

$$\frac{d}{dt}(IKK\ |I \quad |NF \quad)(t) = \ {}_3IKK\ (t) \cdot (I \quad |NF \quad)(t)$$

$$-t_2(IKK\ |I \quad |NF \quad)(t) \tag{B.5}$$

$$\frac{d}{dt} NF \quad (t) = c_{6a}(I \quad |NF \quad)(t) - \ {}_1NF \quad (t) \cdot I \quad (t)$$

$$+t_2(IKK\ |I \quad |NF \quad)(\mathrm{t}) - \ {}_1NF \quad (t) \tag{B.6}$$

$$\frac{d}{dt} NF \quad {}_n(t) = \ {}_1 \ {}_v NF \quad (t) - \ {}_1I \quad {}_n(t) \cdot NF \quad {}_n(t) \tag{B.7}$$

$$\frac{d}{dt} A20(t) = c_4 A20_t(t) - c_5 A20(t) \tag{B.8}$$

$$\frac{d}{dt} A20_t(t) = c_2 + c_1 NF \quad {}_n(t) - c_3 A20_t(t) \tag{B.9}$$

$$\frac{d}{dt} I \quad (t) = - \ {}_2IKK\ (t) \cdot I \quad (t) - \ {}_1I \quad (t) \cdot NF \quad (t) + c_{4a} I \quad {}_t(t)$$

$$-c_{5a} I \quad (t) - \ {}_{1a} I \quad (t) + \ {}_{1a} I \quad {}_n(\mathrm{t}) \tag{B.10}$$

$$\frac{d}{dt} I \quad {}_n(t) = - \ {}_1I \quad {}_n(t) \cdot NF \quad {}_n(t) + \ {}_{1a} \ {}_v I \quad (t) - \ {}_{1a} \ {}_v I \quad {}_n(t) \tag{B.11}$$

$$\frac{d}{dt} I \quad {}_t(t) = c_{2a} + c_{1a} NF \quad {}_n(t) - c_{3a} I \quad {}_t(t) \tag{B.12}$$

$$\frac{d}{dt}(I \quad |NF \quad)(t) = \ {}_1I \quad (t) \cdot NF \quad (t) - c_{6a}(I \quad |NF \quad)(t)$$

$$- \ {}_3IKK\ (t) \cdot (I \quad |NF \quad)(t)$$

$$+ \ {}_{2a}(I \quad {}_n|NF \quad {}_n)(\mathrm{t}) \tag{B.13}$$

$$\frac{d}{dt}(I \quad {}_n|NF \quad {}_n)(t) = \ {}_1I \quad {}_n(t) \cdot NF \quad {}_n(t) - \ {}_{2a} \ {}_v(I \quad {}_n|NF \quad {}_n)(t)$$

$$\tag{B.14}$$

B2 Simulation results of the canonical NF-κB pathway from Lipniacki et al. (2004)

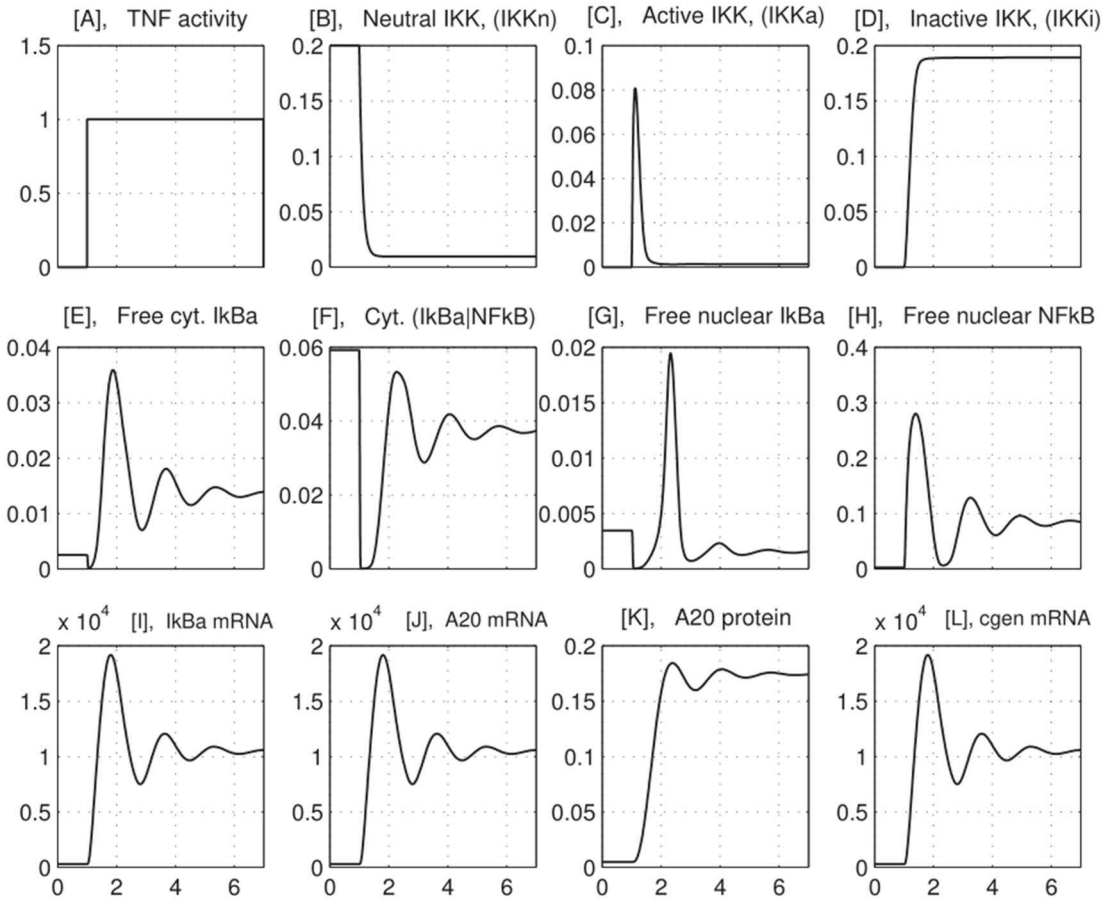

Figure B.1 Numerical Model simulations of the variation in concentrations of biochemical factors regarding the canonical pathway [1].

APPENDIX C

C1 Calculation of model parameters based on GA

The equations of Genetic Algorithm are described as follows:

$$F(\ ) = \sum_{i=1:3}\ b\ (\ \ (\ )_i\ -\ \ _i) \tag{C.1}$$

$$= \tag{C.2}$$

Where X = [n_{1a}, n_{1c}] is a vector that consist of two parameters the value is difficult to know in the model equations. $(\ )_i\ (i = 1,\ 2,\ 3, \dots)$ presents the model outputs based on the vector X corresponding to each point in the parameter space. $E_i(i =$

$1, 2, 3, \ldots)$ presents the target outputs that we want to get corresponding to each point in the parameter space. Our purpose is to minimize $F(\ )$ which is to make model outputs approach to target outputs as much as possible.

REFERENCES

[1] Lipniacki T, Paszek P, Brasier AR, Luxon B, Kimmel M: Mathematical model of NF- κB regulatory module. *Journal of Theoretical Biology* 2004, **228**(2):195-215.

[2] Campbell KJ, Rocha S, Perkins ND: Active repression of antiapoptotic gene expression by RelA(p65) NF-kappa B. *Molecular Cell* 2004, **13**(6):853-865.

[3] Hayden MS, Ghosh S: Shared Principles in NF-κB Signaling. *Cell* 2008, **132**(3):344-362.

[4] Boyce BF, Xiu Y, Li J, Xing L, Yao Z: NF-κB-Mediated Regulation of Osteoclastogenesis. *Endocrinology and Metabolism* 2015, **30**(1):35-44.

[5] Sun SC: Non-canonical NF-κB signaling pathway. *Cell Research* 2011, **21**(1):71-85.

[6] Hoffmann A, Levchenko A, Scott ML, Baltimore D: The IκB-NF-κB Signaling Module: Temporal Control and Selective Gene Activation. *Science* 2002, **298**(5596):1241-1245.

[7] Dejardin E: The alternative NF-kappaB pathway from biochemistry to biology: pitfalls and promises for future drug development. *Biochemical Pharmacology* 2006, **72**(9):1161-1179.

[8] Ghosh S, Karin M: Missing Pieces in the NF-κB Puzzle. *Cell* 2002, **109**(2):S81-S96.

[9] Claudio E, Brown K, Park S, Wang H, Siebenlist U: BAFF-induced NEMO-independent processing of NF-kappa B2 in maturing B cells. *Nature Immunology* 2002, **3**(10):958.

[10] Qing G, Xiao G: Essential role of IkappaB kinase alpha in the constitutive processing of NF-kappaB2 p100. *Journal of Biological Chemistry* 2005, **280**(11):9765-9768.

[11] Karin M, Benneriah Y: Phosphorylation Meets Ubiquitination: The Control of NF-κB Activity. *Annual Review of Immunology* 2003, **18**(1):621.

[12] Endo T, Nishio M, Enzler T, Cottam HB, Fukuda T, James DF, Karin M, Kipps TJ: BAFF and APRIL support chronic lymphocytic leukemia B-cell survival through activation of the canonical NF-kappaB pathway. *Blood* 2007, **109**(2):703-710.

[13] Sun SC, Ley SC: New insights into NF-κB regulation and function. *Trends in Immunology* 2008, **29**(10):469-478.

[14] Vatsyayan J, Qing G, Xiao G, Hu J: SUMO1 modification of NF-kappaB2/p100 is

essential for stimuli-induced p100 phosphorylation and processing. *Embo Reports* 2008, **9**(9):885–890.

[15] Kiran M, Coakley S, Walkinshaw N, Mcminn P, Holcombe M. Validation and discovery from computational biology models. *Biosystems.* 2008, **93**(1):141-150.

[16] Cheong R, Bergmann A, Werner SL, Regal J, Hoffmann A, Levchenko A: Transient IκB Kinase Activity Mediates Temporal NF-κB Dynamics in Response to a Wide Range of Tumor Necrosis Factor-α Doses. *Journal of Biological Chemistry* 2006, **281**(5):2945-2950.

[17] Xue X, Xia W, Hu W. A modeled dynamic regulatory network of NF-κB and IL-6 mediated by miRNA. *BioSystems.* 2013, **114**(3):214-218.

[18] Kim HB, Evans I, Smallwood R, Holcombe M, Qwarnstrom EE. NIK and IKKβ interdependence in NF-κB signalling—Flux analysis of regulation through metabolites. *BioSystems.* 2010, **99**(2):140-149.

[19] Carlotti F, Dower SK, Qwarnstrom EE: Dynamic Shuttling of Nuclear Factor kappa B between the Nucleus and Cytoplasm as a Consequence of Inhibitor Dissociation. *Journal of Biological Chemistry* 2000, **275**(52):41028-41034.

[20] Kearns JD, Basak S, Werner SL, Huang CS, Hoffmann A: IκBε provides negative feedback to control NF-κB oscillations, signaling dynamics, and inflammatory gene expression. *Journal of Cell Biology* 2006, **173**(5):659-664.

[21] Nelson DE, Ihekwaba AEC, Elliott M, Johnson JR, Gibney CA, Foreman BE, Nelson G, See V, Horton CA, Spiller DG: Oscillations in NF-κB Signaling Control the Dynamics of Gene Expression. *Science* 2004, **306**(5696):704-708.

[22] O'Dea EL, Barken D, Peralta RQ, Tran KT, Werner SL, Kearns JD, Levchenko A, Hoffmann A: A homeostatic model of I κ B metabolism to control constitutive NF - κ B activity. *Molecular Systems Biology* 2014, **3**(1):111.

[23] Choudhary S, Kalita M, Fang L, Patel KV, Tian B, Zhao Y, Edeh CB, Brasier AR: Inducible Tumor Necrosis Factor (TNF) Receptor-associated Factor-1 Expression Couples the Canonical to the Non-canonical NF-κB Pathway in TNF Stimulation. *Journal of Biological Chemistry* 2013, **288**(20):14612-14623.

[24] Boyce BF, Xing L: Biology of RANK, RANKL, and osteoprotegerin. *Arthritis Research & Therapy* 2007, **9**(Suppl 1):S1-S1.

[25] Beg AA, Sha WC, Bronson RT, Ghosh S, Baltimore D: Embryonic lethality and liver degeneration in mice lacking the RelA component of NF-kappa B. *Nature* 1995, **376**(6536):167-170.

[26] Hayden MS, Ghosh S: Signaling to NF-κB. *Genes & Development* 2004,

18(18):2195-2224.

[27] Basak S, Behar M, Hoffmann A: Lessons from mathematically modeling the NF-κB pathway. *Immunological Reviews* 2012, **246**(1):221-238.

[28] Wang CY, Mayo MW, Korneluk RG, Goeddel DV, Baldwin AS: NF-κB Antiapoptosis: Induction of TRAF1 and TRAF2 and c-IAP1 and c-IAP2 to Suppress Caspase-8 Activation. *Science* 1998, **281**(5383):1680.

[29] Zheng C, Kabaleeswaran V, Wang Y, Cheng G, Wu H: Crystal structures of the TRAF2: cIAP2 and the TRAF1: TRAF2: cIAP2 complexes: affinity, specificity, and regulation. *Molecular Cell* 2010, **38**(1):101-113.

[30] Al-Sadi R, Guo S, Ye D, Rawat M, Ma TY. TNF-α Modulation of Intestinal Tight Junction Permeability Is Mediated by NIK/IKK-α Axis Activation of the Canonical NF-κB Pathway. *American Journal of Pathology.* 2016, **186**(5):1151-1165.

[31] Yilmaz ZB, Weih DS, Sivakumar V, Weih F. RelB is required for Peyer's patch development: differential regulation of p52–RelB by lymphotoxin and TNF. *The EMBO journal.* 2003, **22**(1):121-130.

[32] Jimi E, Aoki K, Saito H, D'Acquisto F, May MJ, Nakamura I, Sudo T, Kojima T, Okamoto F, Fukushima H: Selective inhibition of NF-kappa B blocks osteoclastogenesis and prevents inflammatory bone destruction in vivo. *Nature Medicine* 2004, **10**(6):617-624.

[33] Basak S, Kim H, Kearns JD, Tergaonkar V, O'Dea E, Werner SL, Benedict CA, Ware CF, Ghosh G, Verma IM: A fourth IκB protein within the NF-κB signaling module. *Cell* 2007, **128**(2):369-381.

FIGURE LEGENDS

Figure 1: The schematic description of two NF-κB pathways for TNF stimulation. (Note that "d" represents the degradation of biochemical factors).

Figure 2: (A) Mimicked changes in the concentrations of TRAF1 mRNA and TRAF2 mRNA with time. (B) Mimicked changes of the variation in the concentrations of TRAF1 and TRAF2 proteins with time. (C) Mimicked changes of variation in the concentration of NIK with time. (D) Mimicked changes of variation in the concentrations of TARF2|NIK, TARF1|NIK and TARF1|TARF2|NIK with time. (E) Mimicked changes of the variation in the concentrations of p100, p52 and p52n with respect to their initial values with time. (F) Mimicked changes of the variation in the concentrations of p50n and p52n with time. (TNF stimulation starts at 5th hour).

Figure 3: (A) Mimicked changes in the concentration of TRAF1 mRNA with time when TNF are set as 0.5, 1 and 1.5 μM respectively. (B) Mimicked changes in the concentration of TRAF2 mRNA when TNF are set as 0.5, 1 and 1.5 μM respectively. (C) Mimicked changes in the concentration of TRAF1 protein with time when TNF are set as 0.5, 1 and 1.5 μM respectively. (D) Mimicked changes in the concentration of TRAF2 protein with time when TNF are set as 0.5, 1 and 1.5 μM respectively. (TNF stimulation starts at 5th hour).

Figure 4: (A) Mimicked changes in the concentration of NIK with time when TNF are set as 0.5, 1 and 1.5 μM respectively. (B) Simulation results demonstrated in (A), but with the short range of the abscissa. (C) Mimicked changes in the concentration of TARF2|NIK with time when TNF are set as 0.5, 1 and 1.5 μM respectively. (D) Simulation results demonstrated in (C), but with the short range of the abscissa. (E) Mimicked changes in the concentration of TRAF1|TARF2|NIK with time when TNF are set as 0.5, 1 and 1.5 μM respectively. (F) Mimicked changes in the concentration of TARF1|NIK with time when TNF are set as 0.5, 1 and 1.5 μM respectively. (TNF stimulation starts at 5th hour).

Figure 5: (A) Mimicked changes in the concentration of p100 with respect to its initial value with time when TNF are set as 0.5, 1 and 1.5 μM respectively. (B) Mimicked changes in the concentration of p52 with respect to its initial value with time when TNF are set as 0.5, 1 and 1.5 μM respectively. (C) Mimicked changes in the concentration of p52n with respect to its initial value with time when TNF are set as 0.5, 1 and 1.5 μM respectively. (D) Mimicked changes in the concentration of p50n with time when TNF are set as 0.5, 1 and 1.5 μM respectively. (TNF stimulation starts at 5th hour).

Figure 6: (A) The effect of independently varying each model parameter (c_{6a} and t_2) on the steady concentration of p50. (B) The effect of independently varying each model parameter (a_1 and i_1) on the steady concentration of p50. (C) The effect of independently varying each model parameter (nc_5, nc_7, nc_8 and nc_9) on the steady concentration of p50. p50 concentration is normalized to the value of the base case.

Figure 7: (A) The effect of independently varying each model parameter (c_{6a}, a_1, t_2 and i_1) on the steady concentration of p52. (B) The effect of independently varying each model parameter (nc_5, nc_7 and nc_8) on the steady concentration of p52. (C) The effect of independently varying each model parameter (nc_9) on the steady concentration of p52. p52 concentration is normalized to the value of the base case.